Turkish Journal of Electrical Engineering & Computer Sciences

http://journals.tubitak.gov.tr/elektrik/

Research Article

Turk J Elec Eng & Comp Sci
(2013) 21: 957 – 979

doi:10.3906/elk-1108-66

A new multiobjective optimal allocation of multitype FACTS devices for total transfer capability enhancement and improving line congestion using the harmony search algorithm

Abbas ESMAEILI, Saeid ESMAEILI*
Department of Electrical Engineering, Shahid Bahonar University of Kerman, Kerman, Iran

Received: 21.08.2011 • **Accepted:** 21.12.2011 • **Published Online:** 03.06.2013 • **Printed:** 24.06.2013

Abstract: In this paper, a new approach based on novel heuristic algorithms is used to locate and model multitype flexible alternating current transmission system (FACTS) devices (series and parallel) in order to improve the total transfer capability and decrease the line congestion and total power loss. The multitype FACTS devices, including the static synchronous series compensator, static compensator, and unified power flow controller, have been optimally sized and located simultaneously through the harmony search algorithm (HSA). To achieve this purpose, a program in MATLAB code has been developed in order to extend the conventional Newton–Raphson algorithm for multitype facts applications. Since the optimization is multipurpose, an analytical hierarchy process is used to obtain the priority vector for each alternative. The HSA, with a good convergence property and more accurate results, can satisfy the objective function better. The effectiveness of the proposed method is demonstrated using a modified 30-bus IEEE test system as well as Iranian 230 kV southeast regional grids in normal and contingency conditions. On the other hand, the optimization performance is compared with a genetic algorithm and particle swarm optimization. The simulation results illustrate that the proposed algorithm performs better than the other algorithms. Moreover, it is shown that simultaneous optimizations of multitype FACTS devices have more advantages than the separate optimization of single-type ones.

Key words: FACTS devices, harmony search algorithm, total transfer capability, lines congestion, analytical hierarchy process, power losses

1. Introduction

In today's power market, there is overgrowing competition in the production and sale of energy. In transmission networks, total transfer capability (TTC) enhancement is one of the major requirements of networks in exchange for increased demand [1,2]. The ability of power systems to provide reliable power transmission can be limited by many factors, such as thermal constraints, voltage, and stability. Therefore, the TTC amount will be limited by overloaded lines and busbars with relatively low voltage [3].

On the other hand, congestion on transmission lines, either in collective or single form, should not exist for more than a few moments, because if the line congestion continues, the power flow equations will diverge. Therefore, system security and reliability will be degraded, and finally the system will collapse. In power systems, it is impossible to fully utilize the transmission line because of different factors, such as voltage limit and stability concerns, that will cause the mitigation of transmittable power to be less than their maximum transmission power, i.e. their thermal limit.

*Correspondence: s_esmaeili@uk.ac.ir

For enhancement of the TTC and accurate management of the congestion in transmission lines, the first option is setting up new transmission lines along with previous transmission lines, but basic barriers ahead of the development of power networks, such as environmental limitations and restrictions of economic issues, will cause the impracticability of the proposal. The second option is using modern compensating equipment of reactive power, i.e. flexible alternating current transmission systems (FACTS) devices [4–6].

FACTS devices, despite minimizing line congestion and maximizing the transfer capability, assure that contractual constraints and targets are satisfied fairly. These devices, with their unique structure, can facilitate in networks the control of power flows in transmission lines. Thus, FACTS devices can improve the stability of transmission lines as well as system security [7].

FACTS devices, compared with conventional approaches such as load shedding and generation rescheduling, seem to be more economical, because these devices, excluding the installation cost, do not impose extra cost at the time of operation [8]. FACTS devices can deal with the controlling active and reactive power simultaneously and they can also monitor the voltage range. Moreover, these devices can lead to a power flow reduction on the overloaded lines by creating an appropriate voltage level. On the other hand, FACTS devices can improve the total voltage stability and also reduce power system losses. A single-type FACTS device belongs to 1 of the 3 groups of FACTS devices, i.e. parallel, series and/or parallel-series devices. Multitype FACTS devices refer to the employment of 2 or more types of FACTS controllers (e.g., 'series and shunt' or 'shunt and combined'). Although using multitype FACTS requires a higher installation cost, it has more advantages for system operating condition improvement than one or more single-type FACTS devices. In addition, multitype FACTS devices can improve some different system parameters in a multiobjective optimization problem. The utilized FACTS devices are a reasonable combination of the new generation of FACTS devices, including the static synchronous series compensator (SSSC) (series), static compensator (STATCOM) (parallel), and unified power flow controller (UPFC) (parallel-series).

Some papers study heuristic approaches and intelligent algorithms to locate FACTS devices in power systems, such as the genetic algorithm (GA) [9] and particle swarm optimization (PSO) method [10], but in most studies carried out in this regard, the locations of the FACTS devices are usually followed up with a single objective. For example, only the increased percentage of the system security limitations and/or the system loadability improvement has been taken into consideration, and in some of these studies, special emphasis has been placed on cost reduction as a main objective [11].

In this paper, through implementing FACTS devices, 3 objectives are followed simultaneously, as follows: 1st objective: increasing total transfer capability, 2nd objective: reducing transmission line congestion, and 3rd objective: reducing system real power losses. This type of formulation was not considered in previous studies.

Here, an approach based on the harmony search algorithm (HSA) is used as a compromise between the contradictory objectives. The HSA is an algorithm that has been inspired for the optimization of issues by a music phenomenon in finding an extraordinary mode from harmony. This algorithm was first presented by Geem et al. in 2001 [12]. In various studies made in this regard, it has been shown that this algorithm operates faster than other similar methods in some complicated optimization methods. The HSA has been successfully applied to various discrete optimization problems such as Sudoku puzzle solving [13] and the traveling salesperson problem [14]. Since the proposed model is the weighted sum of the individual objective functions, an analytical hierarchy process is adopted to specify the weights. It is possible to obtain better results using a multiobjective function, where the improving levels depend on selected weights.

The results achieved by applying the proposed method on a modified IEEE 30-bus test system and Iranian

230 kV southeast regional grid (ISERG) are presented and analyzed as follows. Simulation on these 2 systems has been carried out in both the normal and contingency performance modes. At the end, a comparison of the obtained results with the PSO and GA methods is used to emphasize the proposed method's ability. The results show that the HSA method has significantly increased both the convergence rate and the accuracy of the answers. Hence, the HSA method outperforms other methods.

2. Problem formulation and objective function

In this study, a multiobjective optimization has been considered to find the best capacity and location of the UPFC, SSSC, and STATCOM to satisfy the goal function, which includes 3 objectives: the TTC value, line congestion value, and active power loss value.

2.1. Objective function

As mentioned, the problem is multiobjective optimization, which can be represented as a normalized Eq. (1):

$$\min fit = K_T.\frac{TTC_{normal}}{TTC} + K_c\frac{\sum_{i=1}^{N_{PQ}} W_i.Congestion_i}{\sum_{i=1}^{N_{PQ}} W_i.Congestion_{i,normal}} + K_P\frac{P_{loss}}{P_{loss,normal}} \quad . \tag{1}$$

In Eq. (1), congestion is defined by:

$$\text{Congestion}_i = {S_i}/{S_i^{\max}} \tag{2}$$

where the parameters are defined as follows:

$Congestion_i$: Compression of line i.

P_{loss} : Total active power loss.

S_i : Apparent power flow in line i.

$S_i^{\max}$: Thermal limit of line i.

W_i : Scale coefficients for the compression of line i.

In this paper, the lines that directly affect the TTC have a coefficient equal to 1.5, where the influence of these lines to calculate the total transmission capability is mostly considered. The weighted coefficients of the other grid lines are considered as 1.

Coefficients K_T, K_c, and K_P are the defined weight coefficients of a combined function, which indicates the degree of the individual function in relation to the other functions. In this paper, the analytic hierarchy process (AHP) method is used to obtain these coefficients. To achieve this purpose, Table 1 shows the judge matrix of the above criteria, which reflects the importance and priority criteria toward the other. Here, it is assumed that the TTC is more important than the value of the losses, while the losses have priority over the congestion value.

The final weights of the criteria are obtained using the arithmetic average method [15]. This is as shown in Table 2.

3. Mathematical modeling

In the next section, a mathematical model including the objective function terms and the generalized power flow equations for FACTS devices is illustrated.

Table 1. Criteria's judgeship matrix.

	TTC	Loss	Congestion
TTC	1	3	5
Loss	1/3	1	3
Congestion	1/5	1/3	1

Table 2. Criteria's final weights.

TTC (K_T)	Loss (K_P)	Congestion (K_c)
0.63	0.25	0.12

3.1. Total transfer capability

A framework to determine an interconnected network available transfer capability (ATC) was established by the North American Electric Reliability Corporation for commercially wholesale electricity markets. The ATC consists of the following terms and definitions: the TTC is the maximum transfer power that does not reach the limits and existing transmission commitment (ETC) is the sum of the available transmission commitment between 2 areas. The amount of transmission capability that is required to ensure that the interconnected system is secure under an acceptable range of uncertainty is known as the transmission reliability margin (TRM), and the amount of transmission that is reserved by the load to ensure access to the generation from interconnected systems to meet the requirement of the generation reliability is the capacity benefit margin (CBM). We can then calculate the ATC as:

$$ATC = TTC - TRM - ETC - CBM \tag{3}$$

The determination of the TTC is the main key factor to finding the ATC. The TTC is defined as the maximum increase in the power transfer between the special source/sink areas that transfer without the violation of any security constraints, under both normal and contingency operating conditions.

To calculate the TTC, it is necessary to consider the system's thermal, voltage, and stability limits. Through all of the various methods and algorithms that have been developed, only 3 are applicable for large-scale realistic applications: the repeated power flow (RPF) method [16], continuation power flow method [17], and transfer-based security constrained optimal power flow method.

Among the above methods, the RPF method has several advantages, which include ease of implementation and less convergence time. Hence, in this paper, the RPF method is used to compute the TTC to get reliable results. The next section illustrates the RPF algorithm.

3.2. RPF algorithm

In RPF calculation, the growth in the transmitted power is measured while the complex power increases with a uniform power factor in each load bus in the load area (sink) and the injected real power increases at the generator buses in the generation area (source), step by step, until a violation occurs.

Based on these explanations, the mathematical formulation of the RPF can be used as follows [18]:

Maximize λ
Subject to:

Eq. (4) as equality constraints, which reflects the power flow equations at bus i,

$$\begin{cases} P_{Gi} - P_{Di} - \sum_{j=1}^{n} |V_i|.|V_j|\,|y_{ij}|\cos(\delta_i - \delta_j - \phi_{ij}) = 0 \\ \\ Q_{Gi} - Q_{Di} - \sum_{j=1}^{n} |V_i|.|V_j|\,|y_{ij}|\sin(\delta_i - \delta_j - \phi_{ij}) = 0 \end{cases} . \tag{4}$$

Eqs. (5) and (6) as inequality constraints, which ensures the system voltage and thermal limitations, respectively.

$$|V_i|_{\min} \le |V_i| \le |V_i|_{\max}\,, \tag{5}$$

$$S_{ij} \le S_{ij,\max}. \tag{6}$$

In the above equations, λ is the scalar parameter, representing the increase in the area's load or generation; $\lambda = 0$ is compatible with no transfer (base case); and $\lambda = \lambda_{\max}$ is compatible with the maximum transfer.

P_{Gi}, Q_{Gi} : Real and reactive power generation at bus i.

P_{Di}, Q_{Di} : Real and reactive loads at bus i.

$|V_i|\,, |V_j|$: Voltage magnitude at bus i and bus j.

$|y_{ij}|\,, \phi_{ij}$: Magnitude and phase parts of the ijth element of the bus admittance matrix.

δ_i, δ_j : Voltage angle of bus i and bus j, respectively.

$S_{i,\max}$: Thermal limit of line i.

$|V_i|_{\min}\,, |V_i|_{\max}$: Lower and upper limits of the voltage magnitude at bus i.

S_{ij} : Apparent power flow in line ij.

n : Total number of buses.

In the power flow equations, increases in the generation and demand are applied by the following equations:

$$P_{Gi} = P_{Gi}^0 \times (1 + \lambda.K_{Gi}), \tag{7}$$

$$P_{Di} = P_{Di}^0 \times (1 + \lambda.K_{Di}), \tag{8}$$

$$Q_{Di} = Q_{Di}^0 \times (1 + \lambda.K_{Di}), \tag{9}$$

where

P_{Gi}^0 : Generated initial real power at bus i in the generation area.

P_{Di}^0, Q_{Di}^0 : Initial demanded real and reactive power at bus i in the load area.

K_{Gi}, K_{Di} : Constants used to indicate the change rate in the generation and load as λ alters.

Therefore, the TTC is calculated using Eq. (10) in each case (normal or contingency) as follows:

$$TTC = \textstyle\sum_{i \in SinkArea}^{P_{Di}(\lambda_{\max})} - \sum_{i \in SinkArea}^{P_{Di}^0}, \tag{10}$$

where $\sum_{i \in SinkArea}^{P_{Di}(\lambda_{\max})}$ represents the sink area total load when $\lambda = \lambda_{\max}$ and $\sum_{i \in SinkArea}^{P_{Di}^0}$ represents the sink area total load when $\lambda = 0$.

A schematic flowchart of the computational procedure is shown in Figure 1. In this Figure, when i = 1, values of the TTC, line congestion, and losses are calculated in the base case. In the case of i = 2, these parameters are obtained in the presence of FACTS devices.

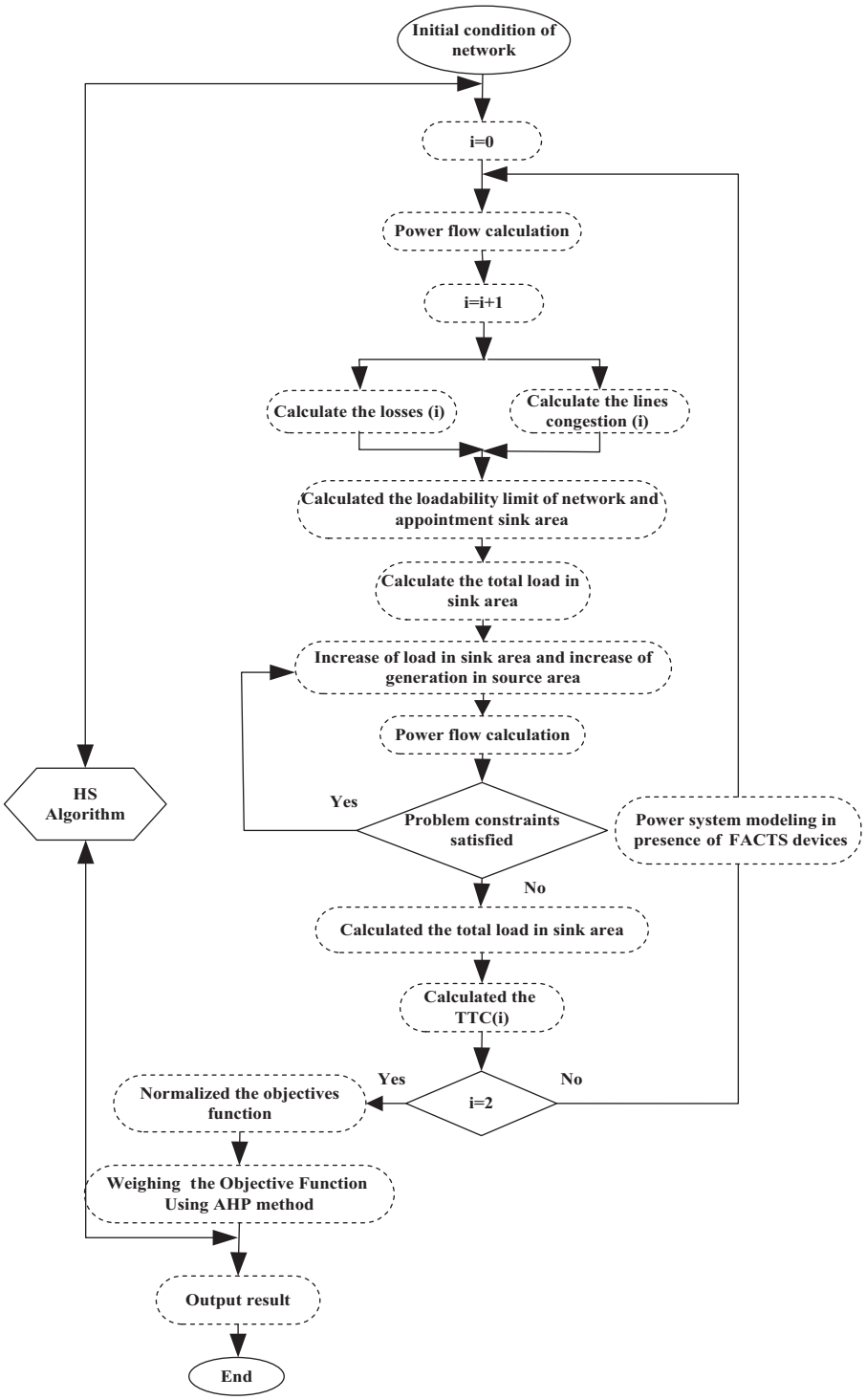

Figure 1. Flowchart of the computational procedure for solving the problem.

4. Modeling of FACTS devices

In this section, we are going to present the useful models of 3 FACTS devices that were used.

4.1. SSSC

The SSSC is a series synchronous voltage type compensator analogous to an ideal electromagnetic generator, which can produce a set of alternating voltages at the desired fundamental frequency with a controllable amplitude and phase angle [19].

If such a series-connected voltage source is located between nodes i and j in a power system, the series voltage source can be modeled with an ideal series voltage V_{se} in the series, with a reactance X_{se}, as shown in Figure 2. V_j models an ideal voltage source and V_i' represents a fictitious voltage behind the series reactance.

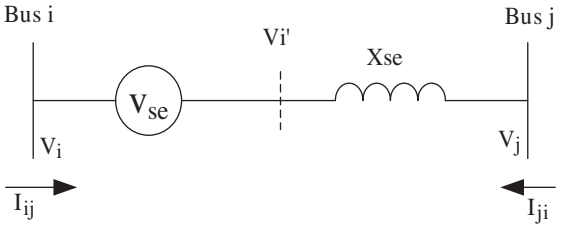

Figure 2. Representation of a series voltage source [25].

The series voltage source V_{se} is controllable in magnitude and phase, i.e. $V_{se} = rV_i e^{j\gamma}$, where $0 < r < r_{\max}$ and $0 < \gamma < 2\pi$. The injection model is obtained by replacing the voltage source by the current source, $I_{se} = -jb_{se}V_{se}$ in parallel with the line, where $b_{se} = 1/X_{se}$ is shown in Figure 3. The injection model for a series-connected voltage source converter is shown in Figure 4.

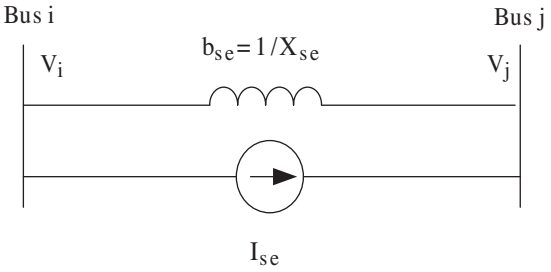

Figure 3. Replacement of voltage source by current source [25].

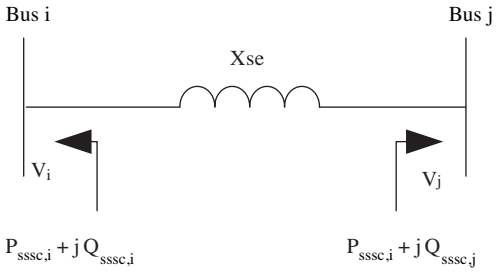

Figure 4. Injection model for a series connected VSC [25].

The current source I_{se} corresponds to the injection powers $S_{i,sssc}$ and $S_{j,sssc}$, where

$$S_{i,sssc} = V_i(-I_{se})^*, \tag{11}$$

$$S_{j,sssc} = V_j(I_{se})^*, \tag{12}$$

The injection power $S_{i,sssc}$ and $S_{j,sssc}$ are simplified to:

$$S_{i,sssc} = V_i[jb_{se}rV_ie^{j\gamma}]^* = b_{se}rV_i^2\sin\gamma - jb_{se}rV_i^2\cos\gamma, \tag{13}$$

$$S_{j,sssc} = -V_j[jb_{se}rV_ie^{j\gamma}]^* = -b_{se}rV_iV_j\sin(\theta_i - \theta_j + \gamma) + jb_{se}rV_iV_j\cos(\theta_i - \theta_j + \gamma), \tag{14}$$

$$P_{i,sssc} = rb_{se}V_i^2 \sin(\gamma), \tag{15}$$

$$P_{j,sssc} = -rb_{se}V_iV_j \sin(\theta_i - \theta_j + \gamma), \tag{16}$$

$$Q_{i,sssc} = -rb_{se}V_i^2 \cos(\gamma), \tag{17}$$

$$Q_{j,sssc} = rb_{se}V_iV_j \cos(\theta_i - \theta_j + \gamma). \tag{18}$$

4.2. The STATCOM

The STATCOM is a second generation FACTS device used in shunt reactive power compensation. The STATCOM is a combination of a voltage sourced converter and an inductive reactance and shunt connected to a power system [20]. The STATCOM circuit is shown in Figure 5. The DC circuit is described by the following differential equations, in terms of the voltage V_{dc} of the capacitor:

$$V_{dc} = \frac{P}{CV_{dc}} - \frac{V_{dc}}{R_CC} - \frac{R(P^2+Q^2)}{CV_i^2V_{dc}}. \tag{19}$$

The power injection at the AC bus that the STATCOM is connected to has the following form:

$$P_{i,STATCOM} = V_i^2G - kV_{dc}V_iG\cos(\theta_i - \alpha) - kV_{dc}V_iB\sin(\theta_i - \alpha), \tag{20}$$

$$Q_{i,STATCOM} = -V_i^2B + kV_{dc}V_iB\cos(\theta_i - \alpha) - kV_{dc}V_iG\sin(\theta_i - \alpha) \tag{21}$$

where

$$k = \sqrt{3/8}m.$$

Hence, the STATCOM device operates to compensate the reactive power only; there must be no active power produced by the device. Therefore, $P_{i,STATCOM} = 0$.

4.3. UPFC

In Figure 6, the focused model of the UPFC is depicted [21]. In this model, the UPFC is considered as 2 voltage source converters, which correspond to the fundamental components of the output voltage of the converters and impedances reflecting the leakage reactances of the 2 coupling transformers.

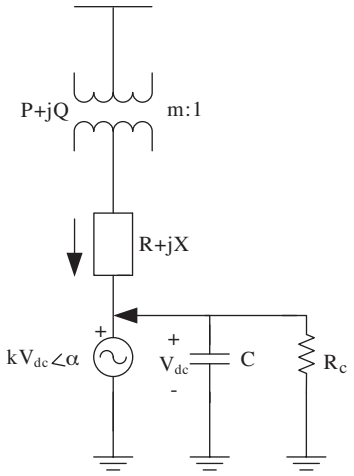

Figure 5. Voltage-source model of STATCOM [26].

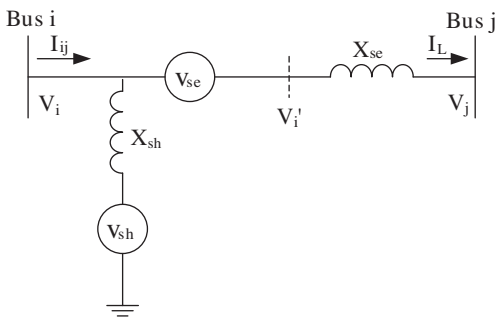

Figure 6. Voltage source model of UPFC [27].

The system voltage is taken as a reference vector $V_i = |V_i| \angle 0$ and $V_i' = V_{se} + V_i$. Both the magnitudes and phase angles of the voltage sources (V_{se}, V_{sh}) are controllable. V_{se} is defined as:

$$V_{se} = rV_i e^{j\gamma}, \tag{22}$$

where

$$0 \le r \le r_{\max} \text{ and } 0 \le \gamma \le 2\pi. \tag{23}$$

The model should be improved by replacing voltage source V_{se} by a current source I_{se}, parallel to the transmission line, similar to a SSSC:

$$I_{se} = -jb_{se}V_{se}, \tag{24}$$

where $b_{se} = 1/X_{se}$.

Hence, in a similar way, the following equation can be extracted for a series converter:

$$P_{is} = -rb_s V_i^2 \sin(\gamma), \tag{25}$$

$$P_{js} = rb_s V_i V_j \sin(\theta_i - \theta_j + \gamma), \tag{26}$$

$$Q_{is} = -rb_s V_i^2 \cos(\gamma), \tag{27}$$

$$Q_{js} = rb_s V_i V_j \cos(\theta_i - \theta_j + \gamma). \tag{28}$$

It is estimated that the total switching losses of the 2 pulse-width modulation converters is about 2% of the transmitted power P_{series}, which should be supplied by a shunt voltage source at bus i. Hence, P_{shunt} is calculated using Eq. (29):

$$P_{shunt} = -1.02P_{series}. \tag{29}$$

In this model converter, 1 is not considered to be a separate controllable shunt reactive source and Q_{shunt} can be assumed to be 0. Based on what was explained, shunt voltage source equivalent power injections can be derived.

The calculation of P_{shunt} can be done using the following formulations:

$$S_{series} = V_{se}I_{ij}^* = re^{j\gamma}V_i(\frac{V_i' - V_j}{jX_{se}})^*. \tag{30}$$

Eq. (30) shows how the active and reactive power supplied by the series converter can be calculated.

$$S_{series} = re^{j\gamma}V_i((re^{j\gamma}V_i + V_i - V_j)/jX_{se})^* \tag{31}$$

$$S_{series} = rV_i e^{j(\theta_i+\gamma)}((rV_i e^{-j(\theta_i+\gamma)} + V_i e^{-j\theta_i} - V_j e^{-j\theta_j})/ - jX_{se}) \tag{32}$$

$$S_{series} = jb_{se}r^2V_i^2 + jb_{se}rV_i^2 e^{j\gamma} - jb_{se}rV_iV_j e^{j(\theta_i-\theta_j+\gamma)} \tag{33}$$

$$S_{series} = jb_{se}r^2V_i^2 + jb_{se}rV_i^2(\cos\gamma + j\sin\gamma) - jb_{se}rV_iV_j(\cos(\theta_i - \theta_j + \gamma) + j\sin(\theta_i - \theta_j + \gamma)) \tag{34}$$

The recent equation can be represented as follows:

$$S_{series} = P_{series} + jQ_{series},$$

where

$$P_{series} = rb_{se}V_iV_j \sin(\theta_i - \theta_j + \gamma) - rb_{se}V_i^2 \sin\gamma, \tag{35}$$

$$Q_{series} = -rb_{se}V_iV_j \sin(\theta_i - \theta_j + \gamma) + rb_{se}V_i^2 \cos\gamma + r^2b_{se}V_i^2. \tag{36}$$

Joining the series and shunt power injections at both bus i and bus j constructs the overall UPFC mathematical model, as shown in Figure 7.

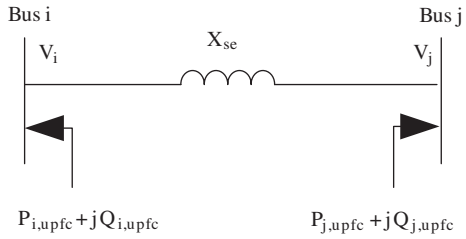

Figure 7. UPFC mathematical model [27].

The elements of the UPFC power injections in Figure 7 are as follows:

$$P_{i,upfc} = P_{is} - 1.02P_{series} = 0.02rb_{se}V_i^2 \sin\gamma - 1.02rb_{se}V_iV_j \sin(\theta_i - \theta_j + \gamma), \tag{37}$$

$$P_{j,upfc} = P_{js} = rb_{se}V_iV_j \sin(\theta_i - \theta_j + \gamma), \tag{38}$$

$$Q_{i,upfc} = 0 + Q_{is} = -rb_{se}V_i^2 \cos\gamma, \tag{39}$$

$$Q_{j,upfc} = Q_{js} = rb_{se}V_iV_j \cos(\theta_i - \theta_j + \gamma). \tag{40}$$

5. Power flow including FACTS devices

The discussed model of the UPFC has been implemented in the conventional Newton–Raphson (NR) power flow algorithm in other references. In this paper, this implementation is generalized for a multitype FACTS application. Accordingly, the general NR equations are presented as follows:

$$P = f_1(V, \theta, G, B), \tag{41}$$

$$Q = f_2(V, \theta, G, B), \tag{42}$$

$$\begin{bmatrix} \Delta P \\ \Delta Q \end{bmatrix}^n = \begin{bmatrix} H & N \\ J & L \end{bmatrix}^n \begin{bmatrix} \Delta\theta \\ \Delta V/V \end{bmatrix}^n, \tag{43}$$

where ΔP and ΔQ are the real and reactive power mismatch vectors; ΔV and $\Delta\theta$ are the vectors of incremental changes in the nodal voltages; H, N, J, and L are the basic elements of the Jacobian matrix; and n is the iteration number. To include FACTS devices in the above formulation, some additional elements of the Jacobian matrix ($(H = H^{org} + H^{facts})$ and for the N, J, and L elements) should be extracted, due to the injections of the FACTS devices at buses $i$and j. These new additional elements are shown in Table 3.

Table 3. Additional elements of the Jacobian matrix including FACTS devices.

Forbus i	when $i=j$	H_{ii}^{facts}	N_{ii}^{facts}	J_{ii}^{facts}	L_{ii}^{facts}
		$\frac{\partial P_{i,facts}}{\partial \theta_i}$	$V_i\frac{\partial P_{i,facts}}{\partial V_i}$	$\frac{\partial Q_{i,facts}}{\partial \theta_i}$	$V_i\frac{\partial Q_{i,facts}}{\partial V_i}$
	when $i\neq j$	H_{ij}^{facts}	N_{ij}^{facts}	J_{ij}^{facts}	L_{ij}^{facts}
		$\frac{\partial P_{i,facts}}{\partial \theta_j}$	$V_j\frac{\partial P_{i,facts}}{\partial V_j}$	$\frac{\partial Q_{i,facts}}{\partial \theta_j}$	$V_j\frac{\partial Q_{i,facts}}{\partial V_j}$
Forbus j	when $i=j$	H_{jj}^{facts}	N_{jj}^{facts}	J_{jj}^{facts}	L_{jj}^{facts}
		$\frac{\partial P_{j,facts}}{\partial \theta_j}$	$V_j\frac{\partial P_{j,facts}}{\partial V_j}$	$\frac{\partial Q_{j,facts}}{\partial \theta_j}$	$V_j\frac{\partial Q_{j,facts}}{\partial V_j}$
	when $i\neq j$	H_{ji}^{facts}	N_{ji}^{facts}	J_{ji}^{facts}	L_{ji}^{facts}
		$\frac{\partial P_{j,facts}}{\partial \theta_i}$	$V_i\frac{\partial P_{j,facts}}{\partial V_i}$	$\frac{\partial Q_{j,facts}}{\partial \theta_i}$	$\frac{\partial Q_{j,facts}}{\partial V_i}$

Furthermore, the power mismatch equations at bus i and bus j must be changed based on the following equations:

$$\Delta P_i = P_{i,G} - P_{i,L} + P_{i,facts} - P_{i,cal}, \tag{44}$$

$$\Delta P_i = P_{j,G} - P_{j,L} + P_{j,facts} - P_{j,cal}, \tag{45}$$

$$\Delta Q_i = Q_{i,G} - Q_{i,L} + Q_{i,facts} - Q_{i,cal}, \tag{46}$$

$$\Delta Q_j = Q_{j,G} - Q_{j,L} + Q_{j,facts} - Q_{j,cal}. \tag{47}$$

The general proposed algorithm for solving the power flow problem including FACTS devices is implemented using MATLAB code. The developed program is referred to as the FACTS devices load flow (FDLF) and is illustrated by the flowchart depicted in Figure 8. The gray and dashed blocks indicate the modification of the conventional NR method.

6. Harmony search algorithm

The HSA originally was inspired by the analogy between music improvisation and the optimization process. Just as musical instruments are played with certain discrete musical notes based on a musician's experiences or the randomness in an improvisation process, so can the design variables be assigned with certain discrete values based on computational intelligence or by randomness in the optimization process [22]. Just as musicians improve their experiences based on an aesthetic standard, the design variables in a computer's memory can be improved based on the fitness function. The original HSA performs based on 5 steps to consider the computational intelligence or randomness as follows:

Step1: Initializing the algorithm parameters.

Step2: Providing the harmony memory (HM).

Step3: Improvising a new harmony.

Step4: Updating the HM.

Step5: Checking the stopping criterion.

The optimum design algorithm using the HSA is sketched basically as shown in Figure 9.

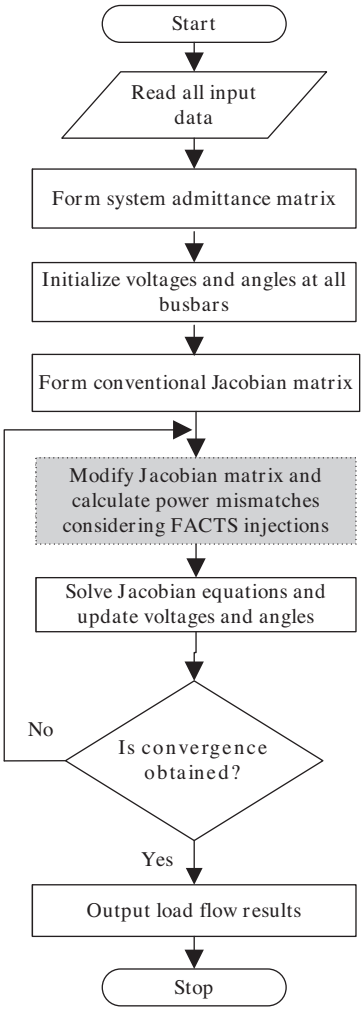

Figure 8. Flow diagram of FDLF.

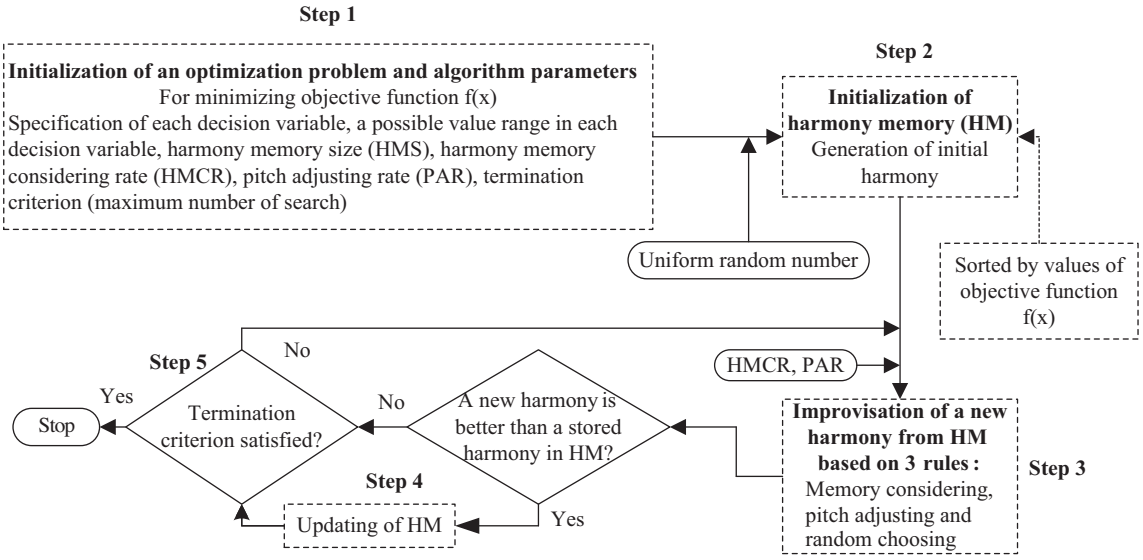

Figure 9. Basic flowchart diagram for the HS algorithm.

Initializing the algorithm parameters and the problem is based on the following problem description:

$$\min(f(x)|x \in X),$$

where f(x) is the main function and x is the set of variables that has the upper bound and lower bound as $x_l < x_i < x_u$. The algorithm parameters that consist of the following parameters are initialized in Step1: the HM size (HMS), or the number of solution vectors in the harmony memory; HM considering rate (HMCR); pitch adjusting rate (PAR); number of decision variables (N); and the number of improvisations (NI) or stopping criterion. The HM is a memory location where all of the solution vectors (sets of decision variables) are stored.

In Step2, to initialize the harmony memory, the HM matrix is filled with as many randomly generated solution vectors as the HMS:

$$HM = \begin{bmatrix} x_1^1 & x_2^1 & \cdots & x_n^1 & f(x^1) \\ x_1^2 & x_2^2 & \cdots & x_n^2 & f(x^2) \\ \vdots & \cdots & \cdots & \cdots & \vdots \\ x_1^{HMS} & x_2^{HMS} & \cdots & x_n^{HMS} & f(x^{HMS}) \end{bmatrix}. \tag{48}$$

In Step3, to improvise a new harmony, 3 rules must be considered, i.e. Rule1: memory consideration, Rule2: pitch adjustment, and Rule3: random selection. To implement Rule1, the value of the first decision variable x_1' for the new vector is selected from any of the values in the specified HM range $(x_1^1 - x_1^{HMS})$. For other variables, we have the same method. The HMCR, which varies between 0 and 1, is defined as the rate of selecting one value from the historical values stored in the HM. Each component obtained by the memory consideration is tested to determine if it should be pitch-adjusted. This operation applies the PAR parameter, which is the rate of the pitch adjustment.

$$x_i' \leftarrow \begin{cases} x_i \in \{x_i^1, x_i^2, x_i^3, ..., x_i^{HMS} & with\ probability\ HMCR\} \\ x_i \in X_i & with\ probablity\ (1 - HMCR) \end{cases} \tag{49}$$

For example, an HMCR = 0.8 indicates that the HSA will choose the decision variable value from historically stored values in the HM, with an 80% probability, or from the entire possible range, with a 20% probability. This operation uses the parameter PAR as follows:

$$x_i' \leftarrow \begin{cases} x_i' \pm rand(0,1).bw & with\ probability\ PAR \\ x_i' & with\ probablity\ (1 - PAR) \end{cases}. \tag{50}$$

where bw is the regularly distributed random number between 0 and 1. Clearly, Step3 is responsible for generating the new potential variation in the algorithm and is comparable to the mutation in standard evolutionary algorithms. Thus, either the decision variable is perturbed with a random number between 0 and bw, it is left unaltered with a probability PAR, or it is left unchanged with probability (1 – PAR).

In Step4, if the new harmony vector, $x' = (x_1', x_2', \ldots, x_N')$, has a better fitness function than the worst harmony in the HM, the new harmony is included in the HM and the existing worst harmony is excluded from the HM. In Step5, the HS algorithm is stopped when the stopping condition (e.g., the maximum number of improvisations) has been satisfied.

Each harmony vector consists of a type of FACTS devices, their values, and locations with specified real numbers. In this structure, FACTS devices including the STATCOM, SSSC, and UPFC can be optimally allocated among specific line/bus candidate locations.

7. Case study and solution results

7.1. IEEE 30 bus test systems

A modified IEEE 30-bus system [23] has been used in this paper to show the effectiveness of the proposed technique to TTC improvement beside congestion disrate at low loss. The test system diagram is shown in Figure 10. The system data are in a per-unit system, where the base MVA value is assumed to be 100 MVA. Three inequality constraints are considered in these studies: the voltage limit, line thermal limit, and reactive power generation limit. The voltage magnitude limit of each bus is assumed to be within 0.95 pu and 1.05 pu. The simulations studies were carried out running on a 2.66 GHz system in a MATLAB 2010a environment.

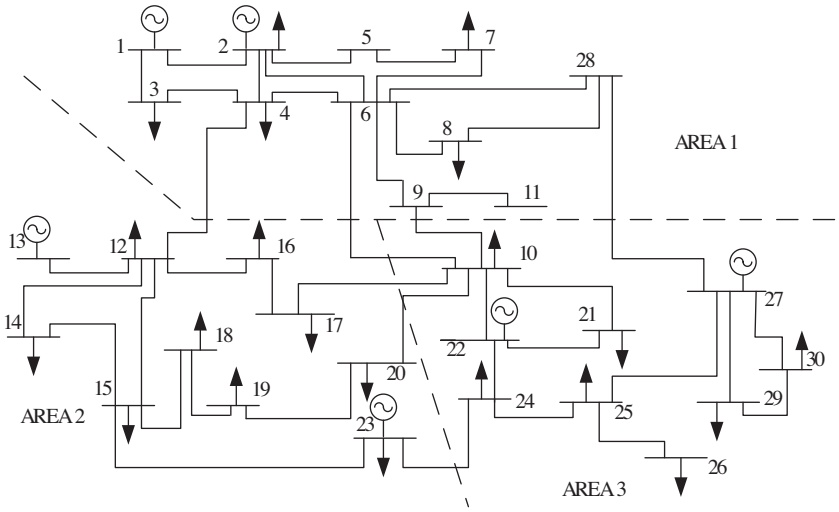

Figure 10. Single diagram of the modified IEEE 30-bus system.

The system has 6 generators and 21 load buses. Bus 1 is the slack bus, and buses 2, 13, 22, 23, and 27 are the real power and voltage magnitude (PV) buses. The system is simulated under normal operating conditions when $\lambda = 0$, to result in the base case value. The RPF is used to make a step increase in the power transfer. The TTC, line congestion, and losses are calculated for the normal and contingency cases.

To calculate the TTC, the low bus and the sink area must be delineating. The network calculations of loadability limit is done using the RPF method. Bus 8 is the weakest system bus, and next buses 7 and 28 are the weakest buses. A diagram of the PV for the weakest buses is shown in Figure 11. In order to effectuate the TTC studies, the system is divided into 3 areas. Bus 8 is in area 1. Thus, area 1 will be considered as the sink area and areas 2 and 3 are the source areas. The TTC for areas 2 to 1 and areas 3 to 1 is computed.

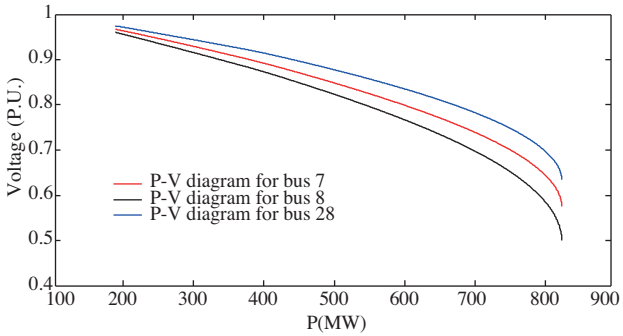

Figure 11. PV diagram for the weakest buses.

The system was tested using 2 FACTS devices installation scenarios: single-type and multitype FACTS devices. The system is simulated in 2 cases: normal operation (without a contingency) and with a contingency, taking into consideration a line outage. To demonstrate the effectiveness of the proposed algorithm and avoid a long computation, only in the case of the multi-FACTS are the HSA results compared to the GA and PSO algorithms. Table 4 displays the HSA, PSO, and GA parameters used for the simulation purposes.

Table 4. Parameters set for the HSA, PSO, and GA.

HS	bw	PAR	HMCR	HMS	NI
	1	0.3	0.9	25	100
PSO	Swarm	c1 = c2	X_{min}	X_{max}	Iterations
	10 * n	2	0.5	1	100
GA	Population	Crossover	Mutation rate	Iterations	
	150	0.8	0.001	100	

7.1.1. Case 1: normal operating conditions

The TTC between areas 2 to 1 and areas 3 to 1 under normal operating conditions without a contingency is 39.38 MW. The total line congestion and total active power loss under normal operating conditions are 8.69 and 2.44 MW, respectively. The simulation results for this stage are shown in Table 5 and the FACTS location and size results are shown in Table 6.

Table 5. Results for the modified IEEE 30-bus system under normal operating conditions.

State	Method	TTC	Congestion	Loss
		Improvement in %		
STATCOM	HSA	37.05	6.2	9.4
SSSC	HSA	24.36	8.1	10.6
UPFC	HSA	42.13	11.35	12.2
Multitype	HSA	54.8	13.7	13.5
Multitype	PSO	52.3	13.1	13.3
Multitype	GA	50.1	12.3	12.9

Table 6. FACTS location and size results.

State	Method	STATCOM		SSSC			UPFC		
		Location (bus)	Q (MVAr)	Location (branch)	r (p.u.)	γ (degree)	Location (branch)	r (p.u.)	γ (degree)
STATCOM	HSA	8	39.1	-	-	-	-	-	-
SSSC	HSA	-	-	8–28	0.93	18	-	-	-
UPFC	HSA	-	-	-	-	-	6–8	0.73	27
Multitype	HSA	17	28.2	12–16	0.84	15	6–8	0.58	24
Multitype	PSO	19	28.6	12–16	0.87	17	6–8	0.56	25
Multitype	GA	8	27.8	12–16	0.86	14	8–28	0.55	21

In single-type devices, it has been shown that the STATCOM, SSSC, and UPFC can be used for TTC enhancement, decreasing line congestion, and minimizing losses. However, compared to the percentage of improvements, the UPFC shows the best performance using the proposed technique. Next to the UPFC, the STATCOM shows better results, because it has a greater impact on improving the voltage profile, which is the main limitation when increasing the TTC. Therefore, the STATCOM can increase the TTC more than the

SSSC. The SSSC has more impact on the power loss and the line congestion also decreases quicker than with the STATCOM, because there is a straightforward relation to improving the line congestion and power loss reductions. Comparing the cost, the STATCOM and SSSC are the best options. Even though the UPFC shows good performance in improving the fitness function, it is more expensive than the STATCOM and SSSC. In multitype FACTS devices, improvement of the fitness function is much better than in single-type devices. In Figures 12 and 13, the bus voltage profile and line congestion profile have been depicted when FACTS devices are present in the system.

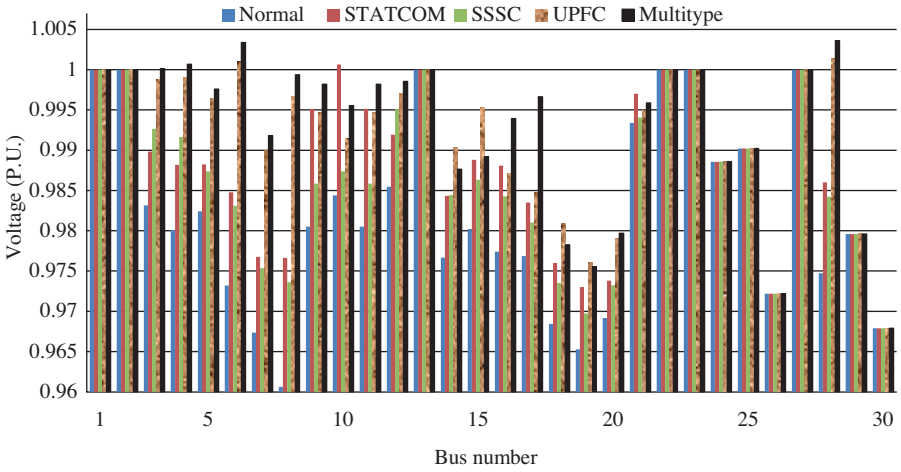

Figure 12. Voltage profiles for different scenarios under normal operating conditions.

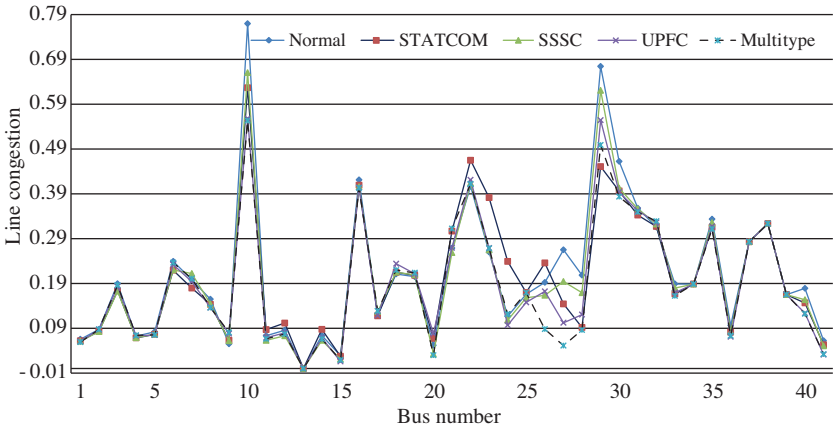

Figure 13. Congestion lines profiles for different scenarios under normal operating conditions.

In all of the cases, it is observed that FACTS devices improve the line power flow to close to its thermal limits and at the same time improve the bus voltage profiles.

7.1.2. Case 2: contingency operating conditions

For a contingency case, the branch line outage between buses 27 and 28 is considered. Thus, the power transfer between areas 1 and 3 is only through the line between buses 9 and 10. At this stage, the TTC without the installation of any FACTS devices is 27.44 MW and bus 8 is the first violated bus. The total line congestion and total active power loss under normal operating conditions is 9.64 and 2.98 MW, respectively. The simulation

results for this stage are shown in Table 7 and the FACTS location and size results are shown in Table 8. The effects of the FACTS devices on the fitness function improvement are more considerable during the contingency case. Using the proposed technique, all of the types of FACTS devices, the STATCOM, SSSC, and UPFC, can be used for TTC enhancement, congestion reduction, and loss reduction. In addition, the fitness function improvement in the contingency case is almost better than that in normal conditions. This shows that in the case of fault conditions, FACTS devices can be used effectively. For the multitype FACTS devices stage, the HSA output is compared with those of the PSO and GA in terms of the objective function for both the normal and contingency cases. However, it is shown that in the contingency case, the UPFC is the best choice for the fitness function improvement. Figures 14 and 15 show the bus voltage and line congestion profile as well.

Table 7. Results for the modified IEEE 30-bus system under contingency operating conditions.

State	Method	TTC	Congestion	Loss
		Improvement in %		
STATCOM	HSA	27.9	2.66	9.3
SSSC	HSA	15.88	5.56	11.7
UPFC	HSA	43.2	9.2	13.4
Multitype	HSA	68.36	10.4	15.4
Multitype	PSO	63.29	10.2	15.24
Multitype	GA	63.84	10.24	15.27

Table 8. FACTS location and size results.

State	Method	STATCOM		SSSC			UPFC		
		Location (bus)	Q (MVAr)	Location (branch)	r (p.u.)	γ (degree)	Location (branch)	r (p.u.)	γ (degree)
STATCOM	HSA	8	43.3	-	-	-	-	-	-
SSSC	HSA	-	-	8–28	0.54	31	-	-	-
UPFC	HSA	-	-	-	-	-	6–8	0. 72	24
Multitype	HSA	24	32.7	8–28	0.49	34	6–10	0.48	37
Multitype	PSO	8	34.1	8–28	0.44	29	6–8	0.41	35
Multitype	GA	8	33.9	8–28	0.44	30	6–10	0.44	31

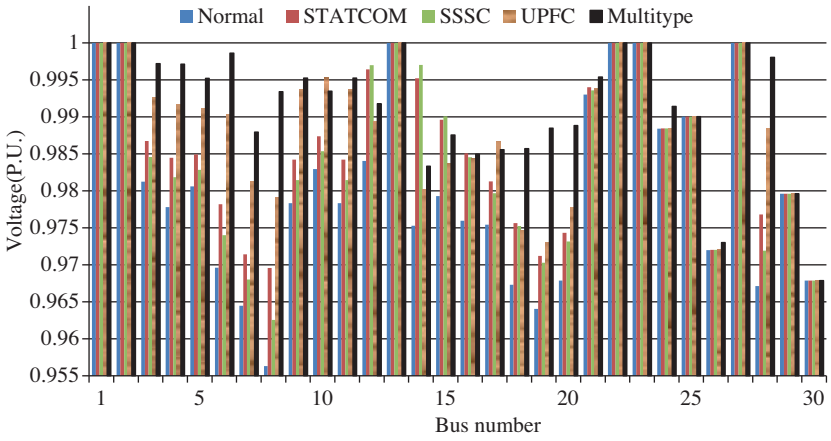

Figure 14. Voltage profiles for different scenarios under contingency operation conditions.

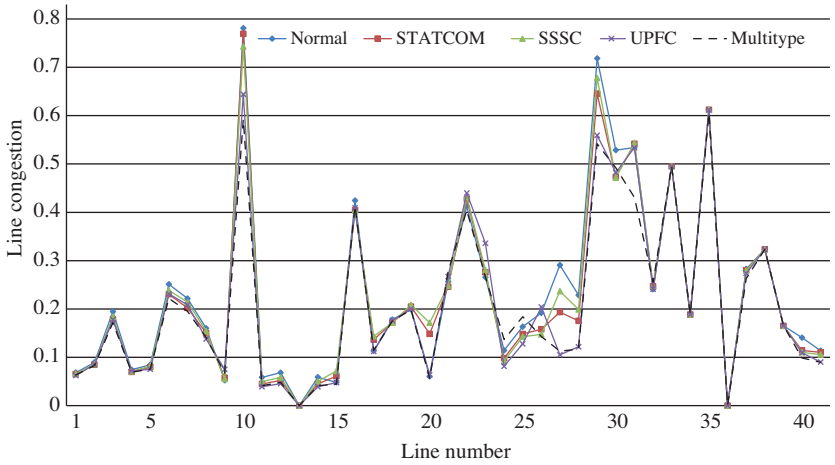

Figure 15. Congestion lines profiles for different scenarios under contingency operation conditions.

7.2. Iranian 230 kV southeast regional grid (2011, operating conditions)

In order to explain the applicability of the proposed algorithm for a real application in a system, a version of Iranian southeast regional grids (ISERG) is used. The systems include 50 buses, 84 lines, and 10 generators, which cover 3 main provinces of Iran. The system total load is about 2344 MW, 1196 MVAr, and the system losses at the base case are 145.8 MW. This network suffers from poor voltage support and line power flow under normal and contingency operating conditions. The diagram of the test system is shown in Figure 16. The solutions for the optimal location of the FACTS devices to maximize the TTC, minimize line congestion, and minimize power losses subject to the voltage limits, line flow limits, and the FACTS device operation limits for this network have been obtained and are discussed below.

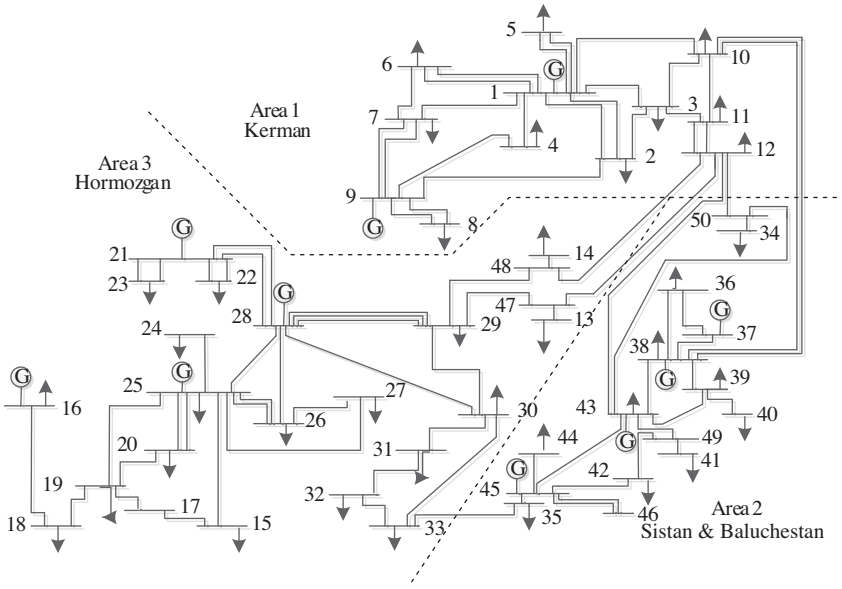

Figure 16. Single-line diagram of Iranian 230 kV southeast regional grid.

This system is also tested in 2 FACTS devices implementation scenarios: single-type and multitype FACTS devices. The system is simulated in 2 cases: normal operating conditions (without a contingency) and with a contingency, taking into consideration the line outage.

Bus 11 is the weakest system bus and the next buses are 12 and 13. The PV diagram for these weakest buses is shown in Figure 17. In order to effectuate the TTC studies, the system is divided into 3 areas. Bus 11 is in area 1. This area will be considered as the sink area, and areas 2 and 3 are the source areas. The TTC for areas 2 to 1 and areas 3 to 1 is computed.

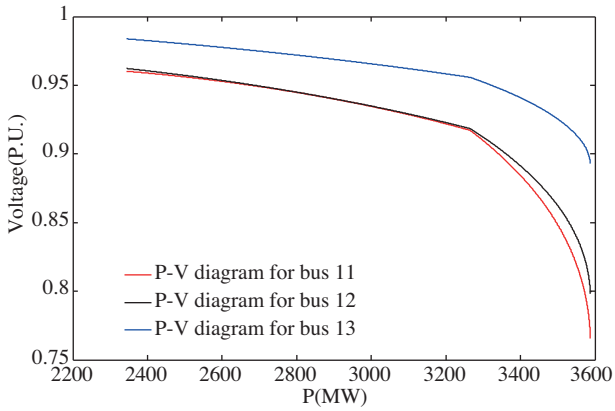

Figure 17. PV diagram for weakest buses.

7.2.1. Case 1: normal operating conditions

The TTC between areas 2 to 1 and areas 3 to 1 under normal operating conditions without any contingency is 268.2 MW, in which bus 11 is the first violated bus. The total line congestion and total active power loss under normal operating conditions is 18.1 and 145.8 MW, respectively. The simulation results for this stage are shown in Table 9 and the FACTS location and size results are shown in Table 10. In the case of the single-type devices, it has been shown that the STATCOM, SSSC, and UPFC have advantages for TTC enhancement, decreasing lines congestion, and minimizing losses. Like the previous test system, the UPFC shows the best performance using the proposed technique. For multitype cases, improvement of the fitness function is much better than in single-type cases. Figures 18 and 19 show the improvement of a bus voltage profile and line congestion profile when FACTS devices are installed in the system. In the ISERG, bus 11 was the weakest bus, and this caused some problems for the downstream 63 kV distribution network. Accordingly, the downstream 63 kV network had low voltage support and high power losses. As is illustrated in Figure 18, the voltage of bus 11 after the installation of the FACTS devices is improved significantly and this problem has been resolved well.

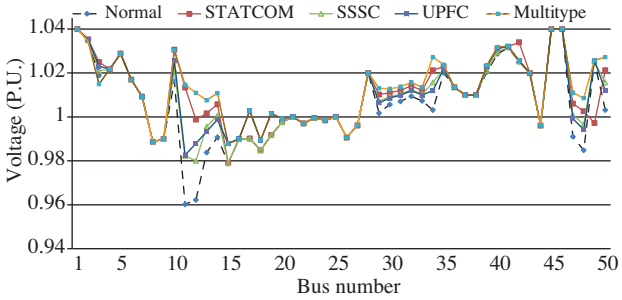

Figure 18. Voltage profiles for different scenarios under normal operating conditions.

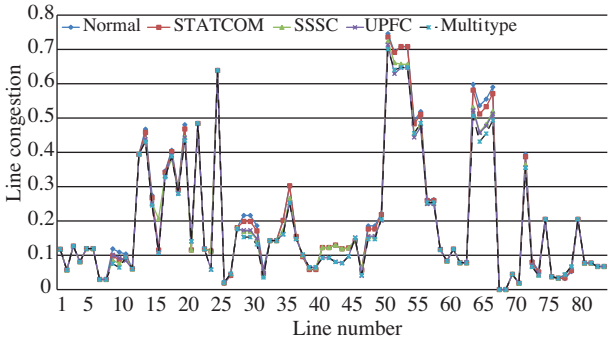

Figure 19. Congestion lines profiles for different scenarios under normal operating conditions.

Table 9. Results for the ISERG under normal operating conditions.

State	Method	TTC	Congestion	Loss
		Improvement in %		
STATCOM	HSA	25.37	2.23	6.65
SSSC	HSA	18.28	5.91	13.1
UPFC	HSA	30.97	8.28	17.4
Multitype	HSA	37.68	10.4	21.6
Multitype	PSO	36.57	10.3	19.8
Multitype	GA	35.98	10.28	19.84

Table 10. FACTS location and size results.

State	Method	STATCOM		SSSC			UPFC		
		Location	Q	Location	r	γ	Location	r	γ
		(bus)	(MVAr)	(branch)	(p.u.)	(degree)	(branch)	(p.u.)	(degree)
STATCOM	HSA	11	87.4	-	-	-	-	-	-
SSSC	HSA	-	-	12–50	0.82	19	-	-	-
UPFC	HSA	-	-	-	-	-	15–17	0.59	43
Multitype	HSA	12	69.3	3–11	0.62	41	15–17	0.48	34
Multitype	PSO	12	67.2	3–11	0.64	37	12–50	0.46	31
Multitype	GA	12	66.9	12–50	0.61	36	12–50	0.47	29

7.2.2. Case 2: contingency operating conditions

For a contingency case, the line outage between buses 12 and 43 is considered. At this stage, the TTC without the installation of any FACTS devices is 198.4 MW and it shows that bus 11 is the first violated bus. The total line congestion and total active power loss under this operating condition are 18.21 and 150.9 MW, respectively. In this step, the results are almost the same as those in the 30-bus test system, which is shown in Table 11, and the FACTS location and size results are shown in Table 12.

Table 11. Results for the ISERG under contingency operating conditions.

State	Method	TTC	Congestion	Loss
		Improvement in %		
STATCOM	HSA	23.3	3.31	11.19
SSSC	HSA	19.4	7.18	17.7
UPFC	HSA	27.6	8.39	20.01
Multitype	HSA	35.6	11.34	24.98
Multitype	PSO	34.2	11.17	24.12
Multitype	GA	32.8	11.04	23.67

However, the effect of the FACTS devices is more considerable for the improvement of the objective functions. In Figures 20 and 21, the voltage and congestion are depicted for different stages, including single- and multitype FACTS devices. For validation of the optimization algorithm, the results obtained by the HSA are compared with the results of other algorithms such as the GA and PSO, in the case of multitype devices. It is obvious that the HSA has a better overall performance than the other 2 methods. It is worth mentioning that the HSA has better computational efficiency than the other methods. To prove this, Figure 22 shows the convergence diagram for the 3 heuristic approaches. It can be seen that the HSA converges in about 37

iterations, while the GA and PSO iterate at 54 and 73, respectively, for convergence to be achieved. This advantage makes a significant reduction in the simulation time for the HSA.

Table 12. FACTS location and size results.

State	Method	STATCOM		SSSC			UPFC		
		Location (bus)	Q (MVAr)	Location (branch)	r (p.u.)	γ (degree)	Location (branch)	r (p.u.)	γ (degree)
STATCOM	HSA	11	92.3	-	-	-	-	-	-
SSSC	HSA	-	-	12-50	0.89	48	-	-	-
UPFC	HSA	-	-	-	-	-	24-25	0.54	44
Multitype	HSA	12	77.2	2-3	0.84	26	20-25	0.51	39
Multitype	PSO	11	73.1	12-50	0.87	24	20-25	0.47	40
Multitype	GA	11	71.9	2-3	0.81	27	20-25	0.45	42

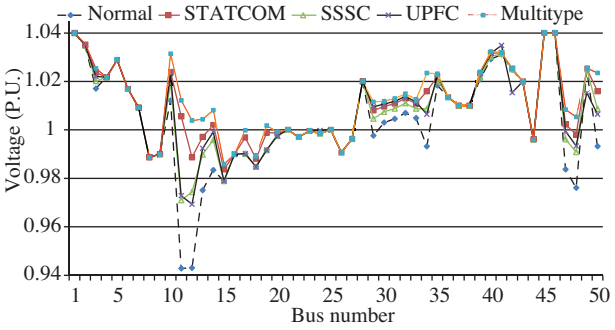

Figure 20. Voltage profiles for different scenarios under contingency operation conditions.

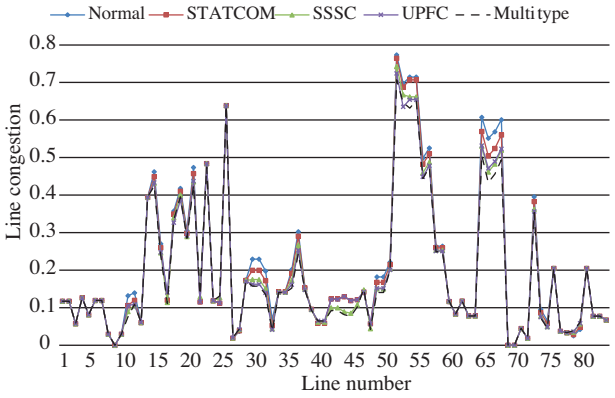

Figure 21. Congestion lines profiles for different scenarios under contingency operation conditions.

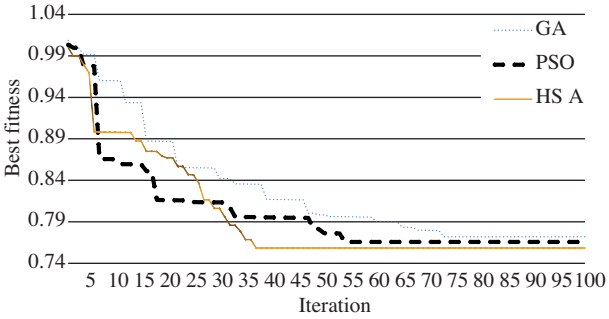

Figure 22. Convergence characteristics of the GA, PSO, and HSA for the best solutions in the placement of multitype FACTS devices stages in the lines outage state.

8. Conclusion

This paper presents an effective method for multitype FACTS device sizing and locating based on a multiobjective function to improve the system operating conditions. Voltage source converter-based FACTS devices, including the STATCOM, SSSC, and UPFC that are discussed here, have parallel, series, and series-parallel

performances, respectively. A perfect multiobjective function consists of increasing the TTC, decreasing line congestion, and minimizing losses, which are formulated for the optimization problem. To achieve this purpose, the AHP makes it possible to rank the objectives in a comparative manner. The optimization of the developed fitness function is performed using a well-known heuristic algorithm named HSA. The proposed algorithms have been implemented on a modified IEEE 30-bus test system and a version of ISERG. The results for normal and contingency operating conditions indicates that the simultaneous allocation and sizing of multitype FACTS devices has more advantages than single-type FACTS to improve the defined terms of the objective functions. To verify the performances of the HSA, some of its results are compared with those obtained using other heuristic methods such as the PSO and GA. The results show better accuracy and convergence characteristics for the HSA in comparison with the GA and PSO.

References

[1] Y. Xiao, Y.H. Song, C. Liu, Y.Z. Sun, "Available transfer capability enhancement using FACTS devices", IEEE Transactions on Power Systems, Vol. 18, pp. 951–954, 2003.

[2] H. Farahmand, M. Rashidinejad, A.A. Gharaveisi, "A combinatorial approach of real GA & fuzzy to ATC enhancement", Turkish Journal of Electrical Engineering & Computer Sciences, Vol. 1, 2007.

[3] North American Electric Reliability Council, "Available transfer capability definition and determination", 1996.

[4] A.A. Edris, "Proposed terms and definitions for FACTS", IEEE Transactions on Power Delivery, Vol. 12, 1997.

[5] P.R. Sharma, A. Kumar, N. Kumar, "Optimal location for shunt connected FACTS devices in a series compensated long transmission line", Turkish Journal of Electrical Engineering & Computer Sciences, Vol. 15, pp. 321–328, 2007.

[6] R.A. Hooshmand, M. Ezatabadi, "Corrective action planning considering FACTS allocation and optimal load shedding using bacterial foraging oriented by particle swarm optimization algorithm", Turkish Journal of Electrical Engineering & Computer Sciences, Vol. 18, pp. 597–612, 2010.

[7] N. Acharya, N. Mithulananthan, "Locating series FACTS devices for congestion management in deregulated electricity markets", Electric Power Systems Research Vol. 77, pp. 352–360, 2007.

[8] W. Shao, V. Vittal, "LP-based OPF for corrective FACTS control to relieve overloads and voltage violations", IEEE Transactions on Power Systems, Vol. 1, pp. 10–30, 2006.

[9] S. Gerbex, R. Cherkaoui, A.J. Germond, "Optimal location of multi-type FACTS devices in a power system by means of genetic algorithms", IEEE Transactions on Power Systems, Vol. 16, pp. 537–544, 2001.

[10] M. Saravanan, S.M.R. Slochanal, P. Venkatesh, J.P.S. Abraham, "Application of particle swarm optimization technique for optimal location of FACTS devices considering cost of installation and system loadability", Electric Power Systems Research, Vol. 77, pp. 276–283, 2007.

[11] B. Gasbaoui, B. Alaoua, "Ant colony optimization applied on combinatorial problem for optimal power flow solution", Leonardo Journal of Sciences, Vol. 14, pp. 1–17, 2009.

[12] Z.W. Geem, "Novel derivative of harmony search algorithm for discrete design variables", Applied Mathematics and Computation, Vol. 19, pp. 223–230, 2008.

[13] Z. Geem, J.Y. Choi, "Music composition using harmony search algorithm", Lecture Notes in Computer Science, Vol. 11, pp. 593–600, 2007.

[14] Z. Geem, "Harmony search algorithm for solving sudoku", Lecture Notes in Artificial Intelligence, Vol. 8, pp. 371–378, 2007.

[15] D.K. Young, T. Younos, R.L. Dymond, D.F. Kibler, D.H. Lee, "Application of the analytic hierarchy process for selecting and modeling storm water best management practices", Universities Council on Water Resources Journal of Contemporary Water Research & Education, Vol. 8, pp. 50–63, 2010.

[16] G.C. Ejebe, J. Tong, J.G. Waight, J.G. Frame, X. Wang, W.F. Tinney, "Available transfer capability calculations", IEEE Transaction on Power Systems, Vol. 13, pp. 1512–1527, 1998.

[17] H. Chiang, A.J. Fluek, K.S. Shah, N. Balu, " CPFLOW: a practical tools for tracing power system steady- state stationary behavior due to load and generation variation", IEEE Transaction on Power Systems, Vol. 10, pp. 1211–1223, 1995.

[18] M.A. Khaburi, M.R. Haghifam, "A probabilistic modeling based approach for total transfer capability enhancement using FACTS devices", Electrical Power and Energy Systems, Vol. 32, pp. 12–16, 2010.

[19] D.M.V. Kumar, "Real-time power system static security enhancement using intelligent - SSSC", Journal of the Institution of Engineers (India). Electrical Engineering Division, Vol. 86, pp. 567–593, 2006.

[20] A. Karami, M. Rashidinejad, A.A. Gharaveisi, "Voltage security enhancement and congestion management via STATCOM & IPFC using artificial intelligence", Iranian Journal of Science & Technology, Vol. 31, pp. 289–301, 2007.

[21] A.M. Vural, M. Tumay, "Mathematical modeling and analysis of a unified power flow controller: a comparison of two approaches in power flow studies and effects of UPFC location", Electrical Power and Energy Systems, Vol. 29, pp. 617–629, 2007.

[22] P. Chakraborty, G.G. Roy, S. Das, D. Jain, "An improved harmony search algorithm with differential mutation operator", Fundamenta Informaticae - Swarm Intelligence, Vol. 95, pp. 1–26, 2009.

[23] R.M Idris, A. Khairuddin, M.W. Mustafa, "Optimal allocation of FACTS devices for ATC enhancement using bees algorithm", World Academy of Science, Engineering and Technology, Vol. 54, pp. 413–421, 2009.